Heliyon

Received:
19 October 2017
Revised:
27 November 2017
Accepted:
28 December 2017

Cite as: Takehito Hayakawa, Yuichi Hatsukawa, Toru Tanimori. ^{95g}Tc and ^{96g}Tc as alternatives to medical radioisotope ^{99m}Tc. Heliyon 4 (2018) e00497. doi: 10.1016/j.heliyon.2017.e00497

^{95g}Tc and ^{96g}Tc as alternatives to medical radioisotope ^{99m}Tc

Takehito Hayakawa [a,*], **Yuichi Hatsukawa** [a], **Toru Tanimori** [b]

[a] *Tokai Quantum Science Center, National Institutes for Quantum and Radiological Science and Technology, Ibaraki 319-1106, Japan*

[b] *Department of Physics, Kyoto University, Kyoto 606-8502, Japan*

* Corresponding author.

E-mail address: hayakawa.takehito@qst.go.jp (T. Hayakawa).

Abstract

We studied ^{95g}Tc and ^{96g}Tc as alternatives to the medical radioisotope ^{99m}Tc. ^{96g}Tc (^{95g}Tc) can be produced by (p, n) reactions on an enriched ^{96}Mo (^{95}Mo) target with a proton beam provided by a compact accelerator such as a medical cyclotron that generate radioisotopes for positron emission tomography (PET). The γ-rays are measured with an electron-tracking Compton camera (ETCC). We calculated the relative intensities of the γ-rays from ^{95g}Tc and ^{96g}Tc. The calculated γ-ray intensity of a ^{96g}Tc (^{95g}Tc) nucleus is as high as 63% (70%) of that of a ^{99m}Tc nucleus. We also calculated the patient radiation doses of ^{95g}Tc and ^{96g}Tc, which were larger than that of ^{99m}Tc by a factor of 2–3 based on the applied assumptions. A medical PET cyclotron which can provide proton beams with energies of 11–12 MeV and a current of 100 μA can produce 12 GBq (39 GBq) of ^{96g}Tc (^{95g}Tc) for operation time of 8 h, which can be used for 240 (200) diagnostic scans.

Keywords: Nuclear physics, Nuclear medicine, Nuclear engineering

1. Introduction

Various radioisotopes, such as ^{99m}Tc (half-life 6.02 h), ^{201}Tl (half-life 3.04 d), and ^{133}Xe (half-life 5.27 d), are used for single-photon emission computed tomography (SPECT) in medical diagnostic scans. In particular, ^{99m}Tc has become the most important medical radioisotope at present [1]. Over 30 commonly used radiopharmaceuticals are based on ^{99m}Tc; in addition, new radiopharmaceuticals

http://dx.doi.org/10.1016/j.heliyon.2017.e00497

have been developed (for example, Refs. [2, 3]). The ^{99m}Tc radioisotopes are supplied by ^{99}Mo/^{99m}Tc generators, which continuously generate ^{99m}Tc through the β-decay of the parent nucleus ^{99}Mo accumulated inside the generators. This supply method provides two excellent advantages. First, it is possible to transport ^{99}Mo/^{99m}Tc generators from a production facility to any place in the world because the half-life of ^{99}Mo is as long as 2.75 d. Second, when a ^{99}Mo/^{99m}Tc generator is transported to a hospital, ^{99m}Tc can be produced fresh for up to 2 weeks by daily milking/elution from this ^{99}Mo/^{99m}Tc generator. At present, the parent nucleus ^{99}Mo is produced in nuclear reactors by the neutron-induced fission of ^{235}U in highly enriched uranium (HEU) targets, in which the fraction of ^{235}U is approximately 90%. However, some nuclear reactors that have supplied ^{99}Mo require major repairs or shutdown, which may lead to a ^{99m}Tc shortage. Thus, many alternative methods to produce ^{99}Mo or ^{99m}Tc without HEU have been proposed [4], and they can be classified into four groups. The first group involves nuclear fission using low-enriched uranium (LEU) with a fraction of up to 20% in nuclear reactors. This technology has been established, and some reactors such as the OPAL reactor [5] have started the production of ^{99}Mo. The second group involves nuclear fission of ^{238}U (or natural uranium) using high-flux neutrons/photons provided by accelerators [6]. This method has two advantages: ^{99m}Tc can be provided in the form of ^{99}Mo/^{99m}Tc generators, and this method does not require LEU or HEU. However, the development of high-flux neutron/photon sources is a technical challenge. The third group involves β-decay from ^{99}Mo produced by nuclear reactions without fission on uranium, for example (n, γ) reactions on ^{98}Mo in nuclear reactors [7], (γ, n) reactions on ^{100}Mo using accelerators [6, 8, 9], or (n, 2n) reaction with high energy neutron beams [10, 11]. The fourth group involves a production process using the ^{100}Mo(p, 2n)^{99m}Tc reaction with proton beams provided by a compact cyclotron with medium energies of 18–24 MeV [12, 13, 14, 15, 16, 17, 18, 19, 20, 21]. For the last two methods, the plan is for ^{99m}Tc to be directly transported from a production facility to hospitals. In such cases, although the half-life of ^{99m}Tc is 6 h, it is expected that a production facility can cover an area with a radius of 400 km [1].

The September 11th terrorist attacks in Washington D.C. in 2001 also affected medical radioisotope production from the viewpoint of the safeguards of nuclear materials. The control of fissionable nuclides such as ^{235}U and ^{239}Pu is important for the safeguards of nuclear materials [22]. The International Atomic Energy Agency (IAEA) hopes to discontinue ^{99m}Tc production using HEU targets, which can be transmuted into nuclear weapons [23]. In the near future, ^{99m}Tc will be supplied by nuclear reactors using LEU targets in addition to HEU. The Nuclear Energy Agency (NEA) reported the prediction that the ^{99}Mo/^{99m}Tc supply will be larger than the world demand when the scheduled nuclear reactors using LEU start ^{99}Mo production [24]. However, the ^{235}U fraction of 20% in LEU is still too high

http://dx.doi.org/10.1016/j.heliyon.2017.e00497

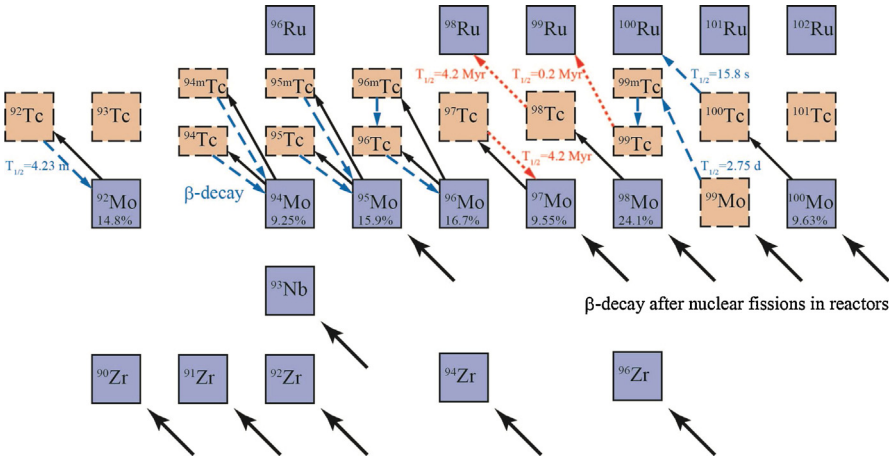

Fig. 1. Partial nuclear chart around Tc isotopes. The solid arrows show the (p, n) reaction. The dashed lines show the β-decays and internal decays with half-lives shorter than 5 days. The dotted lines show the β-decays with half-lives longer than 10^5 years. The large solid arrows show the β-decays after the nuclear fissions in nuclear reactors.

from the viewpoint of the safeguards of nuclear materials. In fact, the governments of the U.S. and Iran agreed to convert Iran's LEU to relatively low-enriched uranium with a fraction of approximately 3.7%, which is usually used for light water reactors. Therefore, the development of an alternative method to supply Tc radioisotopes without LEU or HEU is expected.

Because the Tc chemistry is the same, all the radiopharmaceuticals based on ^{99m}Tc can, in principle, be applied to other Tc isotopes. There are five Tc isotopes with half-lives in the range from hours to days: ^{94m}Tc (half-life 52 m), ^{94g}Tc (half-life 4.88 h), ^{95m}Tc (half-life 60 d), ^{95g}Tc (half-life 20 h), and ^{96g}Tc (half-life 4.28 d), as shown in Fig. 1. Historically, various Tc isotopes have been studied as medical radioisotopes. In 1976, the biological half-life of Tc was measured using ^{95m}Tc instead of ^{99m}Tc [25]. Autoradiography using ^{95m}Tc and ^{96g}Tc was studied in the 1970s [26], and recently, ^{94m}Tc has been studied as a positron emitter for PET [27, 28, 29]. The half-life of ^{96g}Tc (4.28 d) is long enough for worldwide delivery from a production facility and lengthy use of up to 2 weeks in hospitals. ^{95g}Tc (20 h) can also be transported to a wide area and used for 3–5 days in hospitals. Thus, ^{95g}Tc and ^{96g}Tc are candidates for alternative γ-ray emitters. However, the decay rates of ^{95g}Tc and ^{96g}Tc are lower than that of ^{99m}Tc by a factor of 3.3 and 17, respectively, because the decay rate of a radioisotope is inversely proportional to its half-life. This fact leads to the question of whether these isotopes can work as ^{99m}Tc medical radioisotopes.

In the current study, we present the relative γ-ray flux of these isotopes with simple assumptions. We also estimate the patient radiation does per Tc-labeled tracer using the PHITS simulation code [30]. Various nuclear reactions that are

http://dx.doi.org/10.1016/j.heliyon.2017.e00497

production methods of Tc isotopes, such as (p, n) reactions [31, 32, 33], deuteron-induced reactions [34], and ^{96}Ru(n, p)^{96g}Tc reactions [35, 36], were studied. We consider the production by the (p, n) reaction on an enriched Mo isotope. We also calculate the production rate using a typical PET medical cyclotron. Because the energies of decay γ-rays of these Tc isotopes are typically higher than 200 keV, they are not suitable for the traditional SPECT cameras. Thus, we also discuss the property of possible ETCC for high energy γ-rays.

2. Materials and methods

2.1. Relative γ-ray intensity

The question that we should ask here is the γ-ray flux of a Tc isotope relative to that of a ^{99m}Tc nuclide at a detection position outside of a human body. The relative γ-ray flux of a ^{96g}Tc nucleus can be approximately calculated using the equation

$$\mathrm{f}\left({}^{96g}Tc\right) = \frac{\lambda\left({}^{96g}Tc\right)\times R\left({}^{96g}Tc\right)\times M\left({}^{96g}Tc\right)\times I\left({}^{96g}Tc\right)\times P\left({}^{96g}Tc\right)}{\lambda\left({}^{99m}Tc\right)\times R\left({}^{99m}Tc\right)\times M\left({}^{99m}Tc\right)\times I\left({}^{99m}Tc\right)\times P\left({}^{99m}Tc\right)}, \quad (1)$$

where λ is the decay rate of the isotope, R is the decay factor of the isotope during the time between the isotope production and the diagnostic scan, M is the multiplicity of the emitted γ-rays per decay, I is the ratio of the isomer (the ground state) to the summation of the isomer and the ground state at which the nuclides are synthesized in the case that the isomer (the ground state) is used for radiotracers, and P is the probability of the γ-ray penetrating a human body. The aim of the calculation using this simple Eq. (1) is to clearly present the calculation details.

The decay factor R is defined by $R = N_{t1}/N_{t0}$, where N_{t1} and N_{t0} are the numbers of nuclides at the time of a diagnostic scan and at the end of the radioisotope production (beam irradiation or milking), respectively. We assume 1 h as a typical duration for ^{99m}Tc because it is typically produced every morning from ^{99}Mo/^{99m}Tc generators in hospitals, whereas we assume 5 h as a typical duration for the other Tc isotopes that should be transported from production facilities to hospitals.

The multiplicity is the number of γ-rays emitted from a nucleus via decay. As shown in Fig. 2, ^{96g}Tc predominantly decays to two excited states in the daughter nucleus ^{96}Mo through electron capture, and subsequently these two states decay to the ground state by the emission of three cascades of γ-rays with energies of 812 (1127)–850–778 keV. Because the energies of these γ-rays except for the 1127 keV γ-ray are in the narrow energy range of 770–850 keV, it is possible to distinguish the ^{96g}Tc γ-rays with a gate on the energy window of 770–850 keV. We thus take the multiplicity of $M = 3$ for ^{96g}Tc. The nuclear structure of ^{94}Mo is similar to that of ^{96}Mo, and the multiplicity of ^{94g}Tc is also $M = 3$. ^{95m}Tc finally de-excites to the ground state of ^{95}Mo with the emission of various γ-rays

http://dx.doi.org/10.1016/j.heliyon.2017.e00497

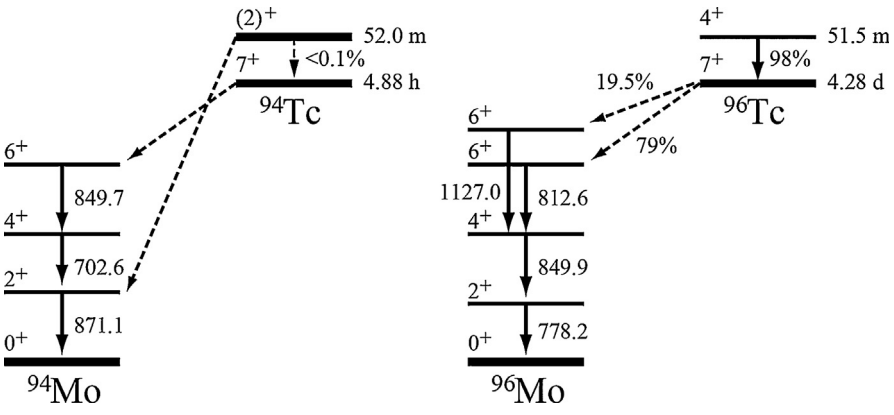

Fig. 2. Partial level schemes for ^{94}Tc (left) and ^{96}Tc (right). The solid arrows with numbers denote decay γ-rays and their energies in unit of keV. The dashed arrows show population from meta-stable states.

following β-decay, and we take $M = 2$ as a typical value for ^{95m}Tc. Because ^{95g}Tc predominantly decays with the emission of a γ-rays of 766 keV, we take a multiplicity of $M = 1$ for ^{95g}Tc.

One point to consider in the calculation of the γ-ray flux is the ratio of the isomer (or the ground state) to the summation of the isomer and the ground state if the isomer (or the ground state) is used for radiotracers. The population ratio of the isomer to the summation for ^{94}Tc is as high as $I(^{94m}\mathrm{Tc}) = 0.8$–$1.0$ and the ratio for ^{95g}Tc is $I(^{95g}\mathrm{Tc}) = 0.25$–$0.3$ [37]. Because the isomer of ^{96}Tc continuously decays to its ground state with a half-life of 52 m during beam irradiation, the final ground ratio depends strongly on the time of the beam irradiation and transport. With assumption of the beam irradiation time of 8 h, the cooling time of 5 h, and the isomer production ratio of $I(^{96m}\mathrm{Tc}) = 0.8$ in proton induced reactions, we obtain $I(^{96g}\mathrm{Tc}) = 0.998$ and $I(^{96m}\mathrm{Tc}) = 0.002$. In the case of the ^{99m}Tc production using the ^{100}Mo(p, 2n)^{99m}Tc reaction, the isomer ratio is approximately 0.3 [38]. When ^{99m}Tc is produced from ^{99}Mo/^{99m}Tc generators, the fraction of ^{99m}Tc is not high because it continuously decays to ^{99g}Tc inside the generators. The fraction of ^{99m}Tc can be calculated as

$$I(^{99m}Tc) = \frac{(\lambda_2 - \lambda_1)(\exp(-\lambda_1 t) - \exp(-\lambda_2 t))}{\lambda_1(1 - \exp(-\lambda_1 t))}, \quad (2)$$

where λ_1 and λ_2 are the decay rates of ^{99}Mo and ^{99m}Tc, respectively, and t is the time interval between two milkings. With the assumption that ^{99m}Tc in saline solution is taken from a ^{99}Mo/^{99m}Tc generator by milking once per day (t = 24 h), the ratio of ^{99m}Tc/(^{99m}Tc + ^{99g}Tc) is 0.38 using Eq. (2). We use an isomer ratio of 0.38 for ^{99m}Tc.

The penetration of γ-rays depends on the depth of the radioisotope and the γ-ray energy. To discuss the γ-ray flux with dependence on the depth, we consider the penetration probability through H_2O with thicknesses of 3 cm and 10 cm.

http://dx.doi.org/10.1016/j.heliyon.2017.e00497

2.2. Dose

To estimate the patient radiation doses from ^{95g}Tc and ^{96g}Tc, we calculated the deposited energy of a ^{95g}Tc (^{96g}Tc) decay using the PHITS particle transport simulation code [30]. The deposited energy depends strongly on the geometry, namely the size of the patient body and the position of the accumulated radiotracers. Here, we assume that the ^{95g}Tc (^{96g}Tc) radioisotopes are located at a 3 cm or 10 cm depth inside a 40-cm diameter sphere that is filled with H_2O. The relative dose is calculated by multiplying the energy deposited in the sphere by the decay rate. The relative doses are obtained as

$$D\left(^{96}Tc\right) = \frac{\lambda\left(^{96}Tc\right) \times I\left(^{96}Tc\right) \times R\left(^{96}Tc\right) \times E\left(^{96}Tc\right)}{\lambda\left(^{99m}Tc\right) \times I\left(^{99m}Tc\right) \times R\left(^{99m}Tc\right) \times E\left(^{99m}Tc\right)}, \quad (3)$$

where E is the deposited energy per decay.

2.3. Production rate using medical compact cyclotron

Compact negative ion cyclotrons for producing various radioisotopes for PET have been developed. These cyclotrons can provide proton beams with currents of up to 100 μA and energies of 12–18 MeV. Furthermore, the advent of cyclotrons with self-radiation shields has enabled the creation of radioisotopes without requiring heavily shielded rooms in hospitals. As a result, over 200 medical PET cyclotrons have already been constructed in Japan. Thus, we consider the (p, n) production using typical medical PET cyclotrons. The (p, n) nuclear reaction cross sections on Mo targets typically have a maximum value in the range of 11–13 MeV. Therefore, medical cyclotrons can effectively produce the radioisotopes ^{95g}Tc/^{96g}Tc. The nuclear reaction cross section depends on the proton beam energy, which decreases via atomic processes inside the targets. Thus, we calculate the production rate with the PHITS code by considering the beam energy loss inside the targets. We assume that a molybdate oxide target with a thickness of 1 g/cm^2 is irradiated by proton beams with energies of 7–15 MeV.

3. Results and discussion

3.1. γ-Ray intensities of ^{95g}Tc and ^{96g}Tc

Table 1 provides a summary of the calculated relative γ-ray intensities and the parameters in the case of a 3-cm thick layer of H_2O. The intensities of ^{96g}Tc and ^{95g}Tc relative to ^{99m}Tc are 0.63 and 0.7, respectively. Table 2 shows the relative intensities in the case of a 10 cm depth, in which the relative intensity of ^{96g}Tc (^{95g}Tc) is 1.0 (1.1). The decay rates of ^{95g}Tc and ^{96g}Tc are much lower than that of ^{99m}Tc. However, the multiplicity, the ground state (isomer) ratio, and the penetrability of ^{95g}Tc (^{96g}Tc) are higher than those of ^{99m}Tc. As a result, the γ-ray

http://dx.doi.org/10.1016/j.heliyon.2017.e00497

Table 1. Relative γ-ray intensity outside of a body.

Isotope	$T_{1/2}$	Decay rate [1/h]	Residual rate after 5 h	Mα	m/(m + g) or g/(m + g)	Penetrability, 3 cm H_2O	Relative intensity
^{99m}Tc[a]	6 h	0.17	0.89[c]	1	0.38[e]	0.63	1.0
^{99m}Tc[b]	6 h	0.17	0.56	1	0.3	0.63	0.50
^{96m}Tc	51.5 m	1.2	0.018	1	0.002[d]	–[f]	–
^{96g}Tc	4.28 d	0.0098	0.97	3	0.998[d]	0.79	0.63
^{95m}Tc	61 d	6.8×10^{-4}	1.0	2	0.25	0.79	7.6×10^{-4}
^{95g}Tc	20 h	0.05	0.84	1	0.75	0.79	0.70
^{94m}Tc	52 m	1.2	0.018	1	0.8	0.80	0.38
^{94g}Tc	4.9 h	0.20	0.49	3	0.2	0.80	1.4

[a] ^{99m}Tc produced by fission in nuclear reactors.

[b] ^{99m}Tc produced by (p, 2n) reactions in accelerators.

[c] Residual rate after 1 h instead of 5 h.

[d] The ratios after the beam irradiation of 8 h and the cooling of 5 h.

[e] See main text.

[f] Internal conversion dominates for the M3 transition with energy of 34 keV.

http://dx.doi.org/10.1016/j.heliyon.2017.e00497

Table 2. Relative γ-ray intensity outside of a body through 10 cm of water.

Isotope	Penetrability, 10 cm H_2O	Relative intensity
^{99m}Tc[a]	0.22	1.0
^{99m}Tc[b]	0.22	0.5
^{96g}Tc	0.46	1.0
^{95m}Tc	0.46	0.013
^{95g}Tc	0.45	1.1
^{94m}Tc	0.47	0.64
^{94g}Tc	0.47	2.3

[a] ^{99m}Tc produced by fission in nuclear reactors.
[b] ^{99m}Tc produced by (p, 2n) reactions in accelerators.

intensity per nucleus becomes almost same. The current results show that ^{96g}Tc and ^{95g}Tc can be used as alternatives to ^{99m}Tc from the viewpoint of the γ-ray flux.

The γ-ray penetrability increases with increasing γ-ray energy in the energy region of $E < 2$ MeV. The penetrability of the 700–900 keV γ-rays from $^{94–96}$Tc through a 10-cm thick layer of H_2O is higher than that of the 141-keV γ-rays from ^{99m}Tc by a factor of approximately 2 (see Table 2). As a result, the relative intensities of these Tc isotopes increase to 1.0–1.1. In this way, these high-energy γ-ray emitters can provide an advantage in the imaging of deep positions in a human body.

3.2. Dose

Tables 3 and 4 show the calculated doses using Eq. (3) and the deposited energies of ^{95g}Tc (^{96g}Tc) decay in the sphere filled with H_2O. Because the decay rates of ^{96g}Tc and ^{95g}Tc are much lower than that of ^{99m}Tc, it is expected that their radiation doses are lower than ^{99m}Tc. However, the calculated doses of ^{95g}Tc and ^{96g}Tc relative to that of ^{99m}Tc are in the range of 2.4–3.0. This is because the total energy of γ-rays emitted from ^{95g}Tc and ^{96g}Tc are as high as 1.1 MeV and 2.5 MeV, respectively, and hence the deposited energy per decay of ^{95g}Tc (^{96g}Tc) is higher than that of ^{99m}Tc by a factor of 5–15. This result suggests that the patient

Table 3. Relative radiation dose in the case of a 3-cm depth.

Isotope	Decay rate [1/h]	Residual rate after 5 h	m/(m + g) or g/(m + g)	Deposited energy [MeV]	Relative dose
^{99m}Tc[a]	0.17	0.89[b]	0.38[c]	0.052	1.0
^{96g}Tc	0.0098	0.97	1	0.88	2.8
^{95g}Tc	0.05	0.84	0.75	0.28	3.0

[a] ^{99m}Tc produced by fission in nuclear reactors.
[b] Residual rate after 1 h instead of 5 h.
[c] See main text.

http://dx.doi.org/10.1016/j.heliyon.2017.e00497

Table 4. Relative radiation dose in the case of a 10-cm depth.

Isotope	Deposited energy [MeV]	Relative dose
^{99m}Tc[a]	0.081	1.0
^{96g}Tc	1.17	2.4
^{95g}Tc	0.38	2.6

[a] ^{99m}Tc produced by fission in nuclear reactors.

radiation doses of ^{95g}Tc and ^{96g}Tc are higher than that of ^{99m}Tc by a factor of approximately 2–3.

Recently, a system combining SPECT and ordinary computed tomography (CT) has been introduced [39]. The radiation dose originating from CT is as high as that of the radiotracer. For example, the radiation is 6.3–8.9 mSv in SPECT/CT scanning using ^{99m}Tc-labled tracers with a radioactivity of 740–1100 MBq, whereas the X-radiation exposure from CT scanning is estimated to be 3.8–15.1 mSv [40]. When ^{95g}Tc or ^{96g}Tc is used as the radiotracer of the SPECT/CT scan, its dose would be higher than that from CT.

3.3. Production rate using medical compact cyclotron

Figs. 4 and 5 show the relative reaction rates calculated with PHITS. In the energy region of $E < 14$ MeV, ^{95g}Tc and ^{95m}Tc are the dominant products of the p + ^{95}Mo reaction (see Fig. 4). Above 14 MeV, the production yields of ^{94g}Tc and ^{94m}Tc, which are produced by (p, 2n) reactions, suddenly increase. The productions of ^{96m}Tc and ^{96g}Tc are dominant at energies of $E < 12$ MeV in the p + ^{96}Mo reaction (see Fig. 5). In both reactions, the production rates of the niobium isotopes are lower than that of the dominant product by at least two orders of magnitude in the energy region of $E \leq 13$ MeV. We conclude that energies of 11–12 MeV are suitable for ^{95g}Tc and ^{96g}Tc production.

During the beam irradiation, ^{96m}Tc with a half-life of 51.5 m continuously decays to ^{96g}Tc. As a result, the residual isomer ratio, m/(m + g), is approximately 13% at the end of the beam irradiation of 8 h. After an additional cooling time of 5 h, the isomer ratio decreases to only 0.2%, whereas the ground state ratio increases to 99.8%. Although the 0.2% fraction of ^{96m}Tc is approximately 20% in activity, due its internal decay it will not cause significant change in the dose to the patients.

For one diagnostic scan, 74–740 MBq of ^{99m}Tc-labeled tracers are injected into a patient. We take 370 MBq as the typical value, corresponding to 1×10^{13} atoms. By dividing by the isomer ratio of ^{99m}Tc/(^{99m}Tc + ^{99g}Tc) = 0.38 (see Table 1), the number of 2.6×10^{13} atoms is obtained as the total number of the ground state and the isomer. As discussed previously, the same number of ^{96g}Tc (^{95g}Tc) atoms can

http://dx.doi.org/10.1016/j.heliyon.2017.e00497

Table 5. Quantities of Tc radioisotopes produced by a proton accelerator. The proton energies are 16 MeV and 11 MeV for ^{99m}Tc and ^{95g}Tc (^{96g}Tc) production, respectively. The irradiation time for ^{95g}Tc (^{96g}Tc) production is 8 h.

Isotopes	^{99m}Tc[a,c]	^{99m}Tc[b,c]	^{95g}Tc[d]	^{95m}Tc[d]	^{96g}Tc[d]	^{96m}Tc[d]
Number of atoms [1/μA]	3×10^{13}	5.1×10^{13}	4×10^{13}	2.1×10^{13}	5.7×10^{13}	7.4×10^{12}
Radioactivity [MBq/μA]	964	1646	390	2.8	110	1700

Note that the isomer ratio ^{99m}Tc/(^{99m}Tc + ^{99g}Tc) decreases to 0.26 and 0.22 for the irradiation time of 3 h and 6 h, respectively [35].

[a] ^{99m}Tc produced by the irradiation time of 3 h.

[b] ^{99m}Tc produced by the irradiation time of 6 h.

[c] These values are taken from Ref. [35], in which the target thickness has been tuned to decrease the proton energy from 16 MeV to 10 MeV.

[d] These values are calculated with a target thickness of 1 g/cm^2 without the cooling time.

work as alternative to ^{99m}Tc from the viewpoint of the γ-ray intensity. By considering the isomer ratio, the radioactivity of the 2.6×10^{13} atoms of ^{96g}Tc (^{95g}Tc) is approximately 49 MBq (190 MBq). In the following discussion, we assume that ^{96g}Tc (^{95g}Tc) isotopes with a radioactivity of 49 MBq (190 MBq) are injected into a patient for a diagnostic scan. When ^{96g}Tc (^{95g}Tc) is produced by a single cyclotron with an irradiation time of 8 h and a reaction rate at 11 MeV, which has been calculated by PHITS, the single cyclotron can produce ^{96g}Tc (^{95g}Tc) with a radioactivity of 12 GBq (39 GBq) each day (see Table 5). These ^{96g}Tc (^{95g}Tc) isotopes can be used for 240 (200) diagnostic scans.

Medical cyclotrons that have been operated to generate radioisotopes for PET can also be employed to generate ^{95g}Tc/^{96g}Tc. A medical PET cyclotron is typically employed for 2 (up to 4) runs per day. The maximum time of each run is 2 h because the half-life of ^{19}F is 2 h, which is the longest among the major radioisotopes for PET. Thus, it is possible to operate these cyclotrons for 8 h per day to generate ^{95g}Tc/^{96g}Tc isotopes. If the beam energy is higher than 12 MeV, the energy can be decreased using metal absorbers. In Japan, more than 200 cyclotrons for PET have already been introduced. 200 cyclotrons can supply ^{96g}Tc (^{95g}Tc) tracers for 48,000 (40,000) diagnostic scans per day. Note that approximately 70,000 treatments using ^{99m}Tc-labeled radiotracers are administered worldwide per day.

3.4. Chemical separation

After the proton beam irradiation, the generated ^{95g}Tc (^{96g}Tc) should be separated from the large excess of molybdenum. Similar technologies have been developed for ^{99m}Tc production using the ^{100}Mo(p, 2n)^{99m}Tc [12, 17, 18, 20], ^{100}Mo(n, 2n)^{99}Mo reactions [11], and ^{94m}Tc production with the ^{94}Mo(p, n)^{94m}Tc reaction [28, 29]: they include thermal separation [11], ion exchange [18, 20], aqueous biphasic

http://dx.doi.org/10.1016/j.heliyon.2017.e00497

extraction chromatography [12], and solid-phase extraction with cross-linked polyethylene glycol resins [17]. Because the chemical behavior of the Tc isotopes is the same, these technologies can be applied to the production of other Tc isotopes from Mo targets. Compact automatic modules for the separation and purification of ^{99m}Tc produced by the ^{100}Mo(p, 2n) reaction have been developed [12, 17, 20], and the use of such automatic modules is feasible.

All the radiopharmaceuticals developed from ^{99m}Tc can, in principle, be produced using the other Tc isotopes if the radionuclide purity and other chemical characteristics are adequate. Various pharmaceutical kits have been developed to produce ^{99m}Tc-labeled tracers from sodium pertechnetate ($Na^{99m}TcO_4$) eluted with saline solution. Thus, if ^{95g}Tc and ^{96g}Tc is delivered to hospitals in the form of sodium pertechnetate with saline solution, various radiotracers can be generated in hospitals using these pharmaceutical kits. In this scheme, ^{95g}Tc (^{96g}Tc) is kept for 3–5 days (2 weeks) in hospitals, in which ^{95g}Tc (^{96g}Tc) continuously decays to ^{95}Mo (^{96}Mo). For example, when ^{96g}Tc is kept for 7 days, approximately 81% of ^{96g}Tc decays to ^{96}Mo. Thus, a chemical procedure to remove Mo from Tc with saline solution should be developed.

3.5. Purity

In the energy region of $E < 12$ MeV, (p, n) reactions are dominant for Mo isotopes (see Figs. 4 and 5); the production of other elements such as niobium is negligible. Thus, when an isotope-enriched Mo target is contaminated with other Mo isotopes, the Tc medical radioisotope is contaminated with other Tc radionuclides produced by (p, n) reactions on the contaminated Mo isotopes (see the solid arrows in Fig. 1). Because the half-lives of ^{92}Tc and ^{100}Tc are as short as 4.23 m and 15.8 s, respectively, they almost entirely decay away during the period from the end of the beam irradiation to a diagnostic scan in hospitals. In contrast, the γ-ray yields of the ^{97}Tc and ^{98}Tc isotopes are relatively small because their half-lives are as long as 4.2×10^6 y and 4.2×10^6 y, respectively. Thus, the radionuclide purity is determined by the factions of the contaminated isotopes of ^{94}Mo, ^{95}Mo, and ^{96}Mo, which can produce $^{94g/94m}$Tc, $^{95g/95m}$Tc, and ^{96g}Tc, respectively. The ^{95}Mo (^{96}Mo) isotope with an enrichment of approximately 97% has been widely used to study nuclear physics [29], in which the fractions of other Mo isotopes are usually lower than 1%. As the enrichment increases, the fraction of the contamination decreases. It should be emphasized that the highly enriched ^{100}Mo targets with a fraction of up to 99.8% have been commercially provided, in which the maximum fraction of contaminated Mo isotopes is 0.17% of ^{98}Mo [16]. If highly enriched ^{95,96}Mo targets are commercially produced, the fraction of contaminated Mo isotopes is expected to be much lower than 1%. Note that the co-production of ^{95m}Tc ($T_{1/2}$ = 61 d) with ^{95g}Tc decreases the purity of ^{95g}Tc, because it is practically impossible

http://dx.doi.org/10.1016/j.heliyon.2017.e00497

to separate ^{95m}Tc and ^{95g}Tc. Thus, ^{96g}Tc is more suitable for the medical radioisotope than ^{95g}Tc.

3.6. γ-Ray imaging

The energies of most γ-rays emitted from Tc isotopes are in the range of 700–1200 keV (see Figs. 2 and 3). In this energy region, Compton scattering is the dominant interaction between photons and atoms. It is thus difficult to image using a detector system coupled with collimators to limit the angle of incident γ-rays, such as the conventional γ-ray detector for the SPECT. Therefore, we need a detector that can reconstruct the Compton scattering event by event. Compton cameras are well-known as such detectors. To determine the direction of an incident γ-ray, in principle, both the angles of the scattered γ-ray and the scattered electron should be measured. However, standard Compton cameras can measure only the angle of the scattered γ-ray. Recently, the ETCC was developed [41, 42, 43, 44, 45, 46]. The ETCC consists of a gaseous time-projection chamber (TPC) coupled to a micro pattern gas detector to measure precisely the track of the recoil electron generated by Compton scattering by an incident photon and a position-sensitive scintillation camera to detect the scattered γ-ray. As a result, the ETCC has an excellent feature: it can measure the angles of both the scattered γ-ray and electron, thereby obtaining the direction of the incident γ-ray. A previous study [41] revealed that the ETCC could provide a clear definition of the point spread function (PSF) and also showed that the standard Compton camera has a PSF of several tens of degrees, whereas the ETCC could give a PSF that is smaller than or equal to ten degrees. Furthermore, Tanimori et al. [43] showed that only the ETCC can perform imaging spectroscopy and that the PSF of the Compton camera intrinsically made this capability difficult due to geometrical optics. Therefore, the ETCC is the most suitable for γ-imaging in the Compton scattering energy region. Hatsukawa et al.

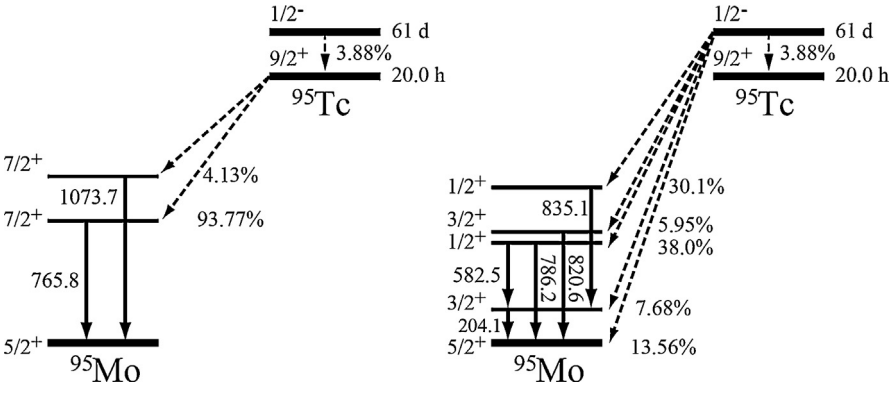

Fig. 3. Partial level schemes for the ground state of ^{95}Tc (left) and the ^{95}Tc isomer (right). The solid arrows with numbers denote decay γ-rays and their energies in unit of keV. The dashed arrows show population from meta-stable states.

http://dx.doi.org/10.1016/j.heliyon.2017.e00497

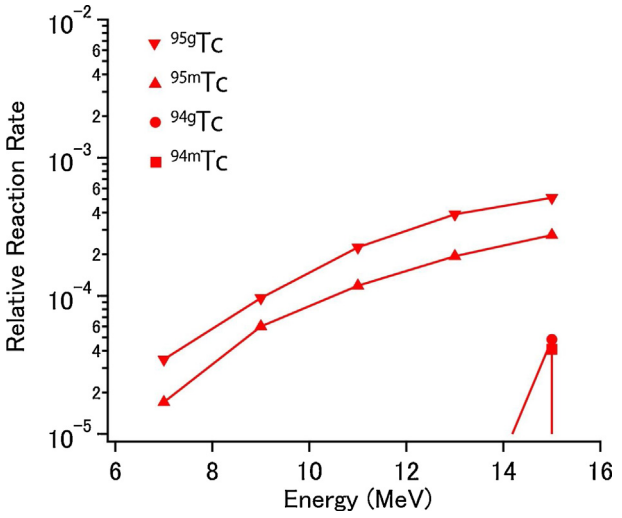

Fig. 4. Calculated relative reaction rates of the p + ^{95}Mo reaction. The thickness of the $^{95}MoO_3$ target is 1 mg/cm^2.

[44] demonstrated the chemical separation of the ^{95m}Tc produced by the ^{95}Mo(p, n) ^{95m}Tc reaction and the measurement of γ-rays from ^{95m}Tc using an ETCC.

We can accurately estimate the imaging performance of the ETCC from the PSF and the detection efficiency of an incident γ-ray. As mentioned in a previous study [43], the detection efficiency and PSF can be precisely estimated using the Compton scattering cross section of the gas and the stopping power of the scintillation detector used in the ETCC due to the simple structure of a cubic gas chamber and an array of scintillator pixels placed at the bottom of the gas chamber. A 30-cm^3 ETCC with a 1-atm Ar gas TPC and one $Gd_2Si_2O_7$:Ce (GSO)

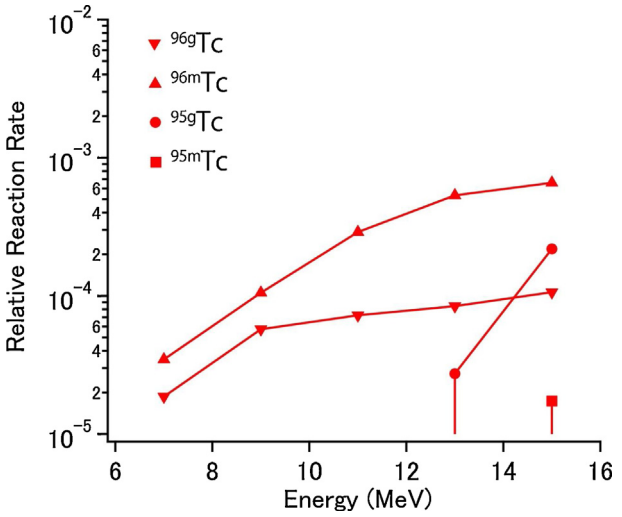

Fig. 5. Calculated relative reaction rates of the p + ^{96}Mo reaction. The thickness of the $^{96}MoO_3$ target is 1 mg/cm^2.

http://dx.doi.org/10.1016/j.heliyon.2017.e00497

scintillation detector array has a PSF of 15 degrees and a detection efficiency of approximately 0.1% for an incident 511-keV γ-ray [42], and a compact 10-cm^3 ETCC with 1.5-atm Ar gas and two GSO scintillator arrays gives a detection efficiency of 0.02% at 511 keV [45].

In 2017, Tanimori et al. expects to release a new type of compact ETCC with a 20-cm diameter-cylindrical TPC with 2-atm Ar gas and two GSO detector arrays, with a detection efficiency of approximately 0.1% at 511 keV [46]. The sensitivity of a γ-ray imaging module is approximately proportional to the detection efficiency and the effective area around a human body. An advantage of the ETCC is that it provides a wide field of view of 3 sr. The construction of ETCC-based γ-ray imaging modules with an effective area of 50% is planned for medical diagnostic scanning. Even if an ETCC module with an effective area of only 25% will be available, its sensitivity for the detection of γ-rays from radiotracers injected into a human body is approximately 200 cps/MBq at 511 keV, where we assume a multiplicity of $M = 1$ and an average penetration probability of 80%. This sensitivity is nearly equal to that of the typical SPECT (190 cps/MBq) [39]. Note that as a final goal of the ETCC, a previous study [41] suggested the possibility that a 30-cm^3 ETCC with 3-atm CF_4 gas will give a detection efficiency of a few % at 511 keV with a good PSF of <3 degrees. This high resolution PSP suggests the sensitivity of a γ-imaging module based on ETCC will be higher than that of the typical SPECT detector by an order of magnitude and the ETCC can provide clearer image. Finally, we would like to stress that the ETCC does not require collimators like SPECT. Thus, it is possible to develop lighter and smaller imaging modules than SPECT.

3.7. Feasibility of ^{96g}Tc and ^{95g}Tc production

The (p, 2n) reaction method [12, 13, 14, 15, 16, 17, 18, 19, 20, 21] and the present proposal have common features that both methods use medical cyclotrons and require the purification of Tc isotopes from Mo targets. Various basic technologies for this (p, 2n) reaction method were developed. As a result, automatic purification modules to separate ^{99m}Tc from a large excess of Mo after the proton beam irradiation were developed [12, 17, 20]. Furthermore, a new process for solid Mo targets based on the electrophoretic deposition of Mo powder onto Ta metal plates was developed [15]. A point for consideration in the economical production of ^{99m}Tc is the recycling of the enriched ^{100}Mo targets after the chemical separation of ^{99m}Tc. However, high recovery yields of $> 90\%$ [12] and 95% [21] have already been achieved. At present, approximately 250 medical cyclotrons with an operating energy of 16.5 MeV, which can produce ^{99m}Tc by the (p, 2n) reaction, have been installed worldwide [19]. Therefore, the (p, 2n) reaction method is feasible for production without the use of either uranium targets or nuclear reactors. Because the chemistry of the separation of ^{99m}Tc from ^{100}Mo and ^{96g}Tc (^{95g}Tc) from ^{96}Mo

http://dx.doi.org/10.1016/j.heliyon.2017.e00497

(^{95}Mo) is, in principle, the same, most technologies developed for the (p, 2n) reaction method can be applied to the ^{96g}Tc (^{95g}Tc) production. However, the ^{96g}Tc (^{95g}Tc) method requires following three technologies. First, we need a new chemical procedure to remove Mo, which is produced via β-decay of Tc, from Tc with saline solution. Second, it is expected that highly enriched ^{95,96}Mo targets with fraction of approximately 99.8% are provided. Third, the ^{96g}Tc (^{95g}Tc) method requires new γ-imaging modules based on the ETCC, but it has two advantages: compactness without collimators and clearer image.

4. Conclusion

^{95g}Tc and ^{96g}Tc are studied as alternatives to the medical radioisotope ^{99m}Tc. The calculated γ-ray intensities of a ^{96g}Tc (^{95g}Tc) nucleus injected into a human body is 63% (70%) relative to that of a ^{99m}Tc nucleus. This result suggests that they can work as γ-ray emitters. ^{96g}Tc (^{95g}Tc) can be produced by (p, n) reactions on enriched ^{96}Mo (^{95}Mo) targets with proton beams provided by compact accelerators such as medical PET cyclotrons. A cyclotron with proton beams with energies of 11–12 MeV and a current of 100 μA can produce 12 GBq (39 GBq) of ^{96g}Tc (^{95g}Tc) for operation of 8 h, which can be used for 240 (200) diagnostic scans. Because the co-production of ^{95m}Tc ($T_{1/2}$ = 61 d) with ^{95g}Tc decreases the purity of ^{95g}Tc, ^{96g}Tc is more suitable for medical radioisotopes than ^{95g}Tc. The estimated patient radiation doses of ^{95g}Tc and ^{96g}Tc are larger than that of ^{99m}Tc by a factor of 2–3 based on the applied assumptions. This method requires the development of a new γ-imaging module based on ETCC, which can provide clearer image than typical SPECT detectors.

Declarations

Author contribution statement

Takehito Hayakawa: Conceived and designed the experiments; Analyzed and interpreted the data; Wrote the paper.

Yuichi Hatsukawa: Analyzed and interpreted the data; Wrote the paper.

Toru Tanimori: Contributed reagents, materials, analysis tools or data; Wrote the paper.

Funding statement

This work was supported by JSPS KAKENHI Grant Numbers JP16K05025 and JP15H03665.

http://dx.doi.org/10.1016/j.heliyon.2017.e00497

Competing interest statement

The authors declare no conflict of interest.

Additional information

No additional information is available for this paper.

References

[1] R. Van Noorden, The medical testing crisis, Nature 504 (2013) 202–204.

[2] Q. Chen, Q. Ma, M. Chen, B. Chen, Q. Wen, B. Jia, et al., An exploratory study on ^{99m}Tc-RGD-BBN peptide scintimammography in the assessment of breast malignant lesions compared to 99mTc-3P4-RGD2, PLoS One 10 (4) (2015) e0123401.

[3] H. Carpenet, A. Cuvillier, J. Monteil, I. Quelven, Anti-CD20 immunoglobulin G radiolabeling with a ^{99m}Tc-tricarbonyl core: in vitro and in vivo evaluations, PLoS One 10 (10) (2015) e0139835.

[4] Review of Potential Molybdenum-99/Technetium-99 m Production Technologies. 2010; 11: Available: https://www.oecd-nea.org/med-radio/supply-series.html.

[5] D. Fraser, Bringing radiochemistry to life. 2013; 12: 3. Available: http://www.ansto.gov.au/AboutANSTO/MediaCentre/News/ACS016995.

[6] H.S. Naik, V. Suryanarayana, K.C. Jagadeesan, S.V. Thakare, P.V. Joshi, V.T. Nimje, et al., An alternative route for the preparation of the medical isotope ^{99}Mo from the ^{238}U(γ, f) and ^{100}Mo(γ, n) reactions, J. Radioanal. Nucl. Chem. 295 (2013) 807–816.

[7] S. Chattopadhyay, S.S. Das, M.K. Das, N.C. Goomer, Recovery of Tc-99 m from Na-2[Mo-99]MoO_4 solution obtained from reactor-produced (n, gamma) Mo-99 using a tiny Dowex-1 column in tandem with a small alumina column, Appl. Radiat. Isot. 66 (2008) 1814–1817.

[8] H. Ejiri, T. Shima, Resonant photonuclear reactions for isotope transmutation, J. Phys. Soc. Jpn. 80 (2011) 094202.

[9] K. Mang'era, K. Ogbomo, R. Zriba, J. Fitzpatrick, J. Brown, E. Pellerin, Processing and evaluation of linear accelerator-produced ^{99}Mo/^{99m}Tc in Canada, J. Radioanal. Nucl. Chem. 305 (2015) 79–85.

[10] Y. Nagai, Y. Hatsukawa, Production of Mo-99 for nuclear medicine by Mo-100(n, 2n)Mo-99, J. Phys. Soc. Jpn. 78 (2009) 033201.

 http://dx.doi.org/10.1016/j.heliyon.2017.e00497

[11] Y. Nagai, Y. Hatsukawa, T. Kin, K. Hashimoto, S. Motoishi, C. Konno, et al., Successful labeling of ^{99m}Tc–MDP using ^{99m}Tc separated from ^{99}Mo produced by ^{100}Mo(n, 2n) ^{99}Mo, J. Phys. Soc. Jpn. 80 (2011) 083201.

[12] T.J. Morley, M. Dodd, K. Gagnon, V. Hanemaayer, J. Wilson, S.A. McQuanrrie, W. English, T.J. Ruth, F. Benard, P. Schaffer, An automated module for the separation and purification of cyclotron-produced $^{99m}Tc_4^-$, Nucl. Med. Biol. 39 (2012) 551–559.

[13] K. Gagnon, J.S. Wilson, C.M.B. Holt, D.N. Abrams, A.J.B. McEwanb, D. Mitlin, S.A. McQuarrie, Cyclotron production of ^{99m}Tc: recycling of enriched ^{100}Mo metaltargets, Appl. Radiat. Isot. 70 (2012) 1685–1690.

[14] O. Lebeda, E.J. van Lier, J. Štursa, J. Ŕalîs, A. Zyuzin, Assessment of radionuclidic impurities in cyclotron produced (99m)Tc, Nucl. Med. Biol. 39 (2012) 1286–1291.

[15] V. Hanemaayer, F. Benard, K.R. Buckly, J. Klug, M. Kovacs, C. Leon, T.J. Ruth, P. Schaffer, S.K. Zeisler, Solid targets for ^{99m}Tc production on medical cyclotrons, J. Radioanal. Nucl. Chem. 299 (2014) 1007–1011.

[16] S.V. Selivanova, É. Lavalĺee, H. Senta, L. Caouette, J.A. Sader, E.J. van Lier, et al., Radioisotopic purity of sodium pertechnetate ^{99m}Tc produced with a medium-energy cyclotron: implications for internal radiation dose, image quality, and release specifications, J. Nucl. Med. 56 (2015) 1600–1608.

[17] F. Bénard, S. Zeisler, M. Vuckovic, K.-S. Lin, Z. Zhang, N. Colpo, T.J. Ruth, P. Schaffer, Cross-linked polyethylene glycol beads to separate ^{99m}Tc-pertechnetate from low specific activity molybdenum, J. Nucl. Med. 55 (2014) 1910–1914.

[18] W. Wojdowska, D. Pawlak, J.L. Parus, R. Mikolajczak, Studies on the separation of ^{99m}Tc from large excess of molybdenum, Nucl. Med. Rev. Cent. East. Eur. 18 (2015) 65–69.

[19] P. Schaffer, F. Benard, A. Bernstein, K. Buckly, A. Celler, N. Cockburn, J. Corsaut, M. Dodd, C. Economou, T. Eriksson, M. Frontera, V. Hanemaayer, B. Hook, J. Klug, M. Kovacs, F.S. Prato, S. McDiarmid, T.J. Ruth, C. Shanks, J.F. Valliant, S. Zeisler, U. Zetterberg, P.A. Zavodszky, Direct production of ^{99m}Tc via ^{100}Mo(p, n) on small medical cyclotrons, Phys. Proc. 66 (2015) 383–395.

[20] M.K. Das, Madhusmita, S. Chattopadhyay, S.S. Das, L. Barua, Md. A. Neyar, U. Kumar, A. De, Production and separation of ^{99m}Tc from cyclotron irradiated $^{100/natural}$Mo targets: a new automated module for separation of ^{99m}Tc from molybdenum targets, J. Radioanal. Nucl. Chem. 310 (2016) 423–432.

 http://dx.doi.org/10.1016/j.heliyon.2017.e00497

[21] P. Trac, G.F. Vandegrift, Recycle of enriched Mo targets for economic production of ^{99}Mo/^{99m}Tc medical isotope without use of enriched uranium, J. Radioanal. Nucl. Chem. 308 (2016) 205–212.

[22] T. Hayakawaw, N. Kikuzawa, R. Hajima, T. Shizuma, N. Nishimori, M. Fujiwara, M. Seya, Nondestructive assay of plutonium and minor actinide in spent fuel using nuclear resonance fluorescence with laser Compton scattering gamma-rays, Nucl. Instrum. Methods Phys. Res. A 621 (2010) 695–700.

[23] Non-HEU Production Technologies for Molybdenum-99 and Technetium-99m, IAEA Nuclear energy series No. NF-T-5.4, 2013; Available at: http://www-pub.iaea.org/books/IAEABooks/10386/Non-HEU-Production-Technologies-for-Molybdenum-99-and-Technetium-99m.

[24] Medical Isotope Supply Review: ^{99}Mo/^{99m}Tc Market Demand and Production Capacity Projection 2016–2021, 2016; 3: 2. Available: https://www.oecd-nea.org/med-radio/supply-series.html.

[25] L. Davis, J. Straw, R.S. Dixon, A. Benedetto, N.L. Sass, Biological half-life of a sup(95m)technetium labeled bone imaging agent, Health Phys. 31 (1976) 521–522.

[26] A. Guillemart, J.-C. Besnard, A. Le Pape, G. Galy, F. Fetissoff, Sketetal uptake of pyrophosphate labeled with technetium-95 m and technetium-96, as evaluated by autoradiography, J. Nucl. Med. 19 (1978) 895–899.

[27] H. Bigott, R. Laforest, X. Liu, A. Ruangma, F. Wuest, M.J. Welch, Advances in the production, processing and microPET image quality of technetium-94m, Nucl. Med. Biol. 33 (2006) 923–933.

[28] C. Hoehr, et al., Radiometals from liquid targets: ^{94m}Tc production using a standard water target on a 13 MeV cyclotron, Appl. Radiat. Isot. 70 (2012) 2308–2312.

[29] B.T. Christian, R.J. Nickles, C.K. Stone, T.L. Mulnix, J. Clark, Improving the radionuclidic purity of ^{94m}Tc for PET imaging, Appl. Radiat. Isot. 46 (1995) 69–73.

[30] T. Sato, K. Niita, N. Matsuda, S. Hashimoto, Y. Iwamoto, S. Noda, T. Ogawa, H. Iwase, H. Nakashima, T. Fukahori, K. Okumura, T. Kai, S. Chiba, T. Furuta, L. Sihver, Particle and heavy ion transport code system PHITS, Version 2.52, J. Nucl. Sci. Technol. 50 (2013) 913–923.

[31] J.J. Hogan, Isomer ratios of Tc isotopes produced in 10–45 MeV bombardments of ^{96}Mo, J. Inorg. Nucl. Chem. 35 (1973) 705–712.

 http://dx.doi.org/10.1016/j.heliyon.2017.e00497

[32] M. Izumo, H. Matsuoka, T. Sorita, Y. Nagame, T. Sekine, K. Hata, et al., Production of 95*m*Tc with proton bombardment of ^{95}Mo, Appl. Radiat. Isot. 42 (1991) 297–301.

[33] F. Tárkányi, F. Ditroi, A. Hermanne, S. Takács, A.V. Ignatyuk, Investigation of activation cross-sections of proton induced nuclear reactions on ^{nat}Mo up to 40 MeV: new data and evaluation, Nucl. Instr. Method. Phys. Res. B 28 (2012) 45–73.

[34] G. Galy, B. Philippon, A. Bardy, R.C. Munsch, Preparation and quality-control of technetium-95 m and technetium-96, Int. J. Appl. Radiat. Isot. 32 (1981) 277–281.

[35] J.H. Zaidi, M. Arif, S. Ahmed, I.H. Qureshi, Measurement of fission neutron spectrum averaged gross sections of some threshold reactions on ruthenium: small scale production of ^{96g}Tc in a nuclear reactor, Radiochim. Acta 85 (1999) 9–12.

[36] J.H. Zaidi, M. Arif, I. Fatima, S. Waheed, S. Ahmad, I.H. Qureshi, Fission spectrum averaged cross section measurements of some neutron threshold reactions of relevance to medical radionuclide production, Radiochim. Acta 93 (2005) 547–552.

[37] B. Strohmaier, M. Fasbender, S.M. Qaim, Production cross sections of ground and isomeric states in the reaction systems ^{93}Nb +^{3}He, ^{92}Mo + α, and $^{94,\ 95}$Mo + *p*, Phys. Rev. C 56 (1997) 2654–2665.

[38] K. Gagnon, F. Ɓenard, M. Kovacs, T.J. Ruth, P. Schaff ; ;er, J.S. Wilson, et al., Cyclotron production of 99*m*Tc: experimental measurement of the ^{100}Mo(p, x)^{99}Mo, ^{99m}Tc and ^{99g}Tc excitation functions from 8 to 18 MeV, Nucl. Med. Biol. 38 (2011) 907–916.

[39] M.T. Madsen, Recent advances in SPECT imaging, J. Nucl. Med. 48 (2007) 661–673.

[40] A.M. Larkin, Y. Serulle, S. Wagner, M.E. Noz, K. Friedman, Quantifying the increase in radiation exposure associated with SPECT/CT compared to SPECT alone for routine nuclear medicine examinations, Int J. Mol. Img. (2011) 897202.

[41] T. Tanimori, H. Kubo, A. Takada, S. Iwaki, S. Komura, S. Kurosawa, et al., An electron-tracking compton telescope for a survey of the deep universe by MeV gamma-rays, Astrophy. J. 810 (2015) 28.

[42] T. Mizumoto, Y. Matsuoka, Y. Mizumura, T. Tanimori, H. Kubo, A. Takada, et al., New readout and data-acquisition system in an electron-tracking

 http://dx.doi.org/10.1016/j.heliyon.2017.e00497

Compton camera for MeV gamma-ray astronomy (SMILE-II), Nucl. Instr. Method. Phys. Res. A 800 (2015) 40–50.

[43] T. Tanimori, et al., Establishment of imaging spectroscopy of nuclear gamma-rays based on geometrical optics, Sci. Rep. 7 (2017) 41511.

[44] Y. Hatsukawa, K. Hashimoto, K. Tsukada, T. Sato, M. Asai, A. Toyoshima, Y. Nagai, T. Tanimori, S. Sonoda, S. Kabuki, H. Saji, H. Kimura, Production of ^{95m}Tc for Compton camera imaging, J. Radioanal. Nucl. Chem. 303 (2015) 1283–1285.

[45] T. Mizumoto, et al., A performance study of an electron-tracking Compton camera with a compact system for environmental gamma-ray observation, J. Instrum. 10 (2015) C01053.

[46] D. Tomono, et al., First on-site true gamma-ray imaging-spectroscopy of contamination near Fukushima plant, Sci. Rep. 7 (2017) 41972.

 http://dx.doi.org/10.1016/j.heliyon.2017.e00497